IEEE Access
Multidisciplinary | Rapid Review | Open Access Journal

Received 1 June 2024, accepted 10 June 2024, date of publication 13 June 2024, date of current version 21 June 2024.

Digital Object Identifier 10.1109/ACCESS.2024.3413824

RESEARCH ARTICLE

Channel Modeling for IRS-Assisted MIMO Systems to Analyze the Effects of Nonlinear Distortions in Wireless Environments

D. L. SHARINI, RAVILLA DILLI, (Member, IEEE), M. KANTHI, (Member, IEEE), AND G. D. GOUTHAM SIMHA, (Member, IEEE)

Department of Electronics and Communication Engineering, Manipal Institute of Technology, Manipal Academy of Higher Education, Manipal, Karnataka 576104, India

Corresponding author: Ravilla Dilli (dilli.ravilla@manipal.edu)

ABSTRACT B5G networks are envisioned to meet higher spectral efficiencies through advanced transmission technologies. Consequently, it is important to comprehend the typical propagation characteristics of wireless communication medium that experience multipath effects, fading, shadowing, and nonlinear distortions. Most of these challenging issues arise under non-line of sight conditions concerning the propagation medium, which deteriorates the quality of the signal received due to uncontrollable channel variations. The recent advances in Intelligent Reflecting Surface (IRS), enable a dynamically alterable wireless environment to achieve flexible reconfigurable channels. The deployment of IRS can evidently bypass the obstacles through smart reflections and shall mitigate channel fading impairments. Motivated by the potentials of the IRS, this paper investigates the performance of IRS-assisted multi-input-multi-output (MIMO) systems to analyze the effect of nonlinear distortions and system adaptation over IID and non-IID Gaussian channel variations. The simulations show the distortion levels with the help of power spectral density for correlated or uncorrelated channel conditions. Furthermore, Monte Carlo simulations are performed to understand the behavior of the wireless system through the analysis of bit error rate (BER) vs signal-to-noise ratio (SNR), Ergodic Channel capacity vs SNR in the presence of IID-Gaussian/ non-IID Gaussian and in-band nonlinear distortions. Additionally, in realistic channel conditions, it is observed that the effect of increasing the number of IRS elements increases the BER performance of ∼8dB in both IID and non-IID Gaussian variations. Finally, improvement in the performance of ergodic capacity of 5 bps/Hz has been observed at a fixed SNR of 5dB.

INDEX TERMS B5G, bit error rate, ergodic channel capacity, intelligent reflecting surface, IID Gaussian, non-IID Gaussian, MIMO, M-QAM, NLOS, nonlinear distortion.

I. INTRODUCTION

IRS-assisted MIMO system ideates to fuse into the future B5G wireless communication to escalate the spectral/ energy efficiencies. This integration provides myriad opportunities for improving performance by cautiously tuning the phase shifts of the signal transmitted from the base station so that the signal reaches the receiver without experiencing many blockages, loss, or interference [1]. The strategic placement of such a system provides flexibility to deploy in any environmental scenarios that constitute better signal penetration through a high density of users by confining the signals within specific areas [2]. Nonetheless, IRS-assisted MIMO systems encounter several design challenges that can compromise their capacity and performance [3]. Some of these challenges include the effect of nonlinear distortion that add on to the channel during signal transmission where it tends to dwindle the system SNR and hence, bit error rate at the receiver. Thus,

The associate editor coordinating the review of this manuscript and approving it for publication was Irfan Ahmed.

''channel modelling'' serves a critical function in examining the intricate behaviours exhibited by channels, encompassing noise attributes, distortion, and other factors, some of which may clearly introduce nonlinearity.

The primary distinction between linear and nonlinear characteristics within the channel lies in the observable alterations of the signal spectrum's structure or shape in linear scenarios [4]. However, nonlinearity initiates certain effects on the signal spectrum where the ''probability distribution'' of signal parameters deviates from Gaussian distribution producing non-IID Gaussian noise [4], [5]. Thus, accurate knowledge of noise characteristics is very beneficial in understanding theoretical limits for data transmission as these noise components suffer from correlated realizations [5]. Significantly, whenever correlation exists between noise samples, it induces distortion and ISI, that impacts the performance of the communication channel [6]. In case, if the signal lacks correlation or is ''uncorrelated'' with the expected signal, it is deemed as uncorrelated distortions. These distortions are treated as noise components akin to AWGN [7]. Additionally, the phase of the radio wave introduces phase jitter and distortion in the received signal [8]. It is essential to note that, phase noise in the wireless channel alone does not yield a non-IID Gaussian process. If the phase noise conforms to a Gaussian distribution, the resulting signal will still remain IID Gaussian. However, if the phase noise introduces nonlinear distortion, distribution follows non-IID Gaussian [9].

Furthermore, comprehending the impacts of nonlinear distortions utilizing the nonlinear model referred in [10], [11], [12], and [13], emphasizes on ''uncorrelated distortion component''. Here, the uncorrelated component comprises ''in-band'' and ''out-of-band'' distortion. These in-band distortions result in the deterioration of SNR, while out-of-band distortions lead to ACI. The power of these uncorrelated components relies on envelope variations of signal transmission and PAPR. Thus, various modulation schemes induce distinct amounts of nonlinear distortion and this results in affecting BER differently.

Besides, literature in [14], [15], [16], and [17], has incorporated nonlinearities through devices namely power amplifiers, mixer circuits, equalizers, frequency multipliers, and, so on. These devices lead to intermodulation products, spectral regrowth, and amplitude or phase distortions. Authors in [18], [19], [20], and [21] demonstrated how the phase distortions lead to an error in the decoded symbols, resulting in a rapid increase of BER. In [22], authors examined the effects of ''transmit nonlinearity'' caused by multicarrier amplifiers in MISO systems where it is illustrated how intermodulation distortions were reduced by proper allocation of frequency. Authors in [23] utilized a constellation view to understand nonlinearity is manifested as ''rotation/ compression'' of the signal, interpreting nonlinear distortion that accounts for a higher probability of error.

The major contributions of this article include:

- Investigate the BER performance of IRS based spatial multiplexing system in IID Gaussian, non-IID Gaussian channels and analyze the performance over nonlinear distorted channels
- Performance analysis in typical outdoor and indoor channels with the augmentation of IRS.
- Analyze the ergodic channel capacity for MIMO based spatial multiplexing systems under various channel perturbations and nonlinear distortions.

A. ORGANIZATION AND NOTATIONS

The article is organized as follows. Section II illustrates system and channel model, with algorithmic development of MIMO SMX systems in IRS scenarios. Simulation results are provided in section III and section IV concludes the paper.

The main notations are as follows. The operators $|\cdot|$, $\|\cdot\|$ denote the absolute value and vector norms, whereas $exp\,(x)$ and $\log_2(x)$ respectively stands for exponential and logarithm functions. Additionally, $\sqrt{x}$, diag (x), and I stand for square root of x, diagonal matrix with x on the main diagonal and Identity matrix with suitable dimension respectively. The ''transpose'' and ''conjugate transpose'' of matrix H are denoted as H^T and H^H respectively. $\Gamma(\cdot)$ indicates Gamma function. Table 1 provides the list of acronyms used in the article.

TABLE 1. List of acronyms used.

Acronym	Description
ACI	Adjacent Channel Interference
AWGN	Additive White Gaussian Noise
B5G	Beyond fifth Generation
BER	Bit Error Rate
CLT	Central Limit Theorem
FT	Fourier Transform
IID	Independent and identically distributed
IRS	Intelligent Reflecting Surface
ISI	Inter Symbol Interference
LOS	Line of Sight
MIMO	Multiple Input Multiple Output
MISO	Multiple Input Single Output
NLOS	Non-Line of Sight
PAPR	Peak to Average Power Ratio
PSD	Power Spectral Density
QoS	Quality of Service
RIS	Reconfigurable intelligent surface
SMX	Spatial Multiplexing
SNR	Signal to Noise Ratio
SISO	Single Input Single Output
THz	Terahertz

II. MODELING

A. SYSTEM AND CHANNEL MODEL

This section presents the system and channel model of IRS based spatial multiplexing system over nonlinear distorted channels. Despite the advances in MIMO technologies, the purpose of incorporating IRS with MIMO attempts to deliver an effective phase shift Ø to achieve flexible reconfigurable channels and ceases the drawbacks of signal interference in conventional MIMO technologies.

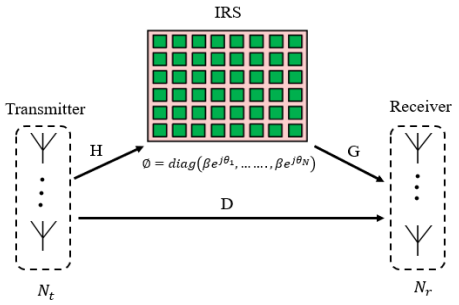

FIGURE 1. IRS- aided MIMO communication system.

These phase shifts generated by (IRS_{ele}) IRS reflecting elements constitute to diagonal matrix $\emptyset_{N\times N}$ as shown in Figure 1 that captures complex reconfigurable responses of IRS elements which is represented using Equation 1 of [24].

$$\emptyset = diag\left(\beta e^{j\theta_1}, \ldots\ldots, \beta e^{j\theta_N}\right) \tag{1}$$

From Equation 1, $\theta \in [0, 2\pi)$ and β denotes the phase shift matrix and reflection coefficient. Considering β =1 helps in acquiring maximal signal reflections [24]. Furthermore, the signal reflected from N_t transmit antennas via IRS channels experience the effect of nonlinear distortions over correlated or uncorrelated channel conditions. Specifically, some degree of spatial correlation is expected to occur among IRS elements, which evidently influences the performance limits.

$$H = \gamma \sum_{c=1}^{C} \sum_{s=1}^{S} \beta \sqrt{G_e\left(\theta^{T-RIS}\right) L^{T-RIS}} a \times \left(\emptyset^{T-RIS}, \theta^{T-RIS}\right) a^T \left(\emptyset^{Tx}, \theta^{Tx}\right) + H_{LOS} \tag{2}$$

$$G = \bar{\gamma} \sum_{c=1}^{\bar{C}} \sum_{s=1}^{\bar{S}} \bar{\beta} \sqrt{G_e\left(\theta^{RIS-R}\right) L^{RIS-R}} a\left(\emptyset^{Rx}, \theta^{Rx}\right) \times a^T \left(\emptyset^{RIS-R}, \theta^{RIS-R}\right) + G_{LOS} \tag{3}$$

$$D = \tilde{\gamma} \sum_{c=1}^{\bar{C}} \sum_{s=1}^{\bar{S}} \tilde{\beta} \sqrt{L^{T-R} a}\left(\emptyset^{Rx'}, \theta^{Rx'}\right) a^T \left(\emptyset^{Tx'}, \theta^{Tx'}\right) + D_{LOS} \tag{4}$$

For the illustration, channel between ''transmitter to IRS'' is mathematically given as channel matrix coefficient H (H $\epsilon C^{N\times N_T}$), G (G $\epsilon C^{N_R\times N}$) denotes for ''IRS to the receiver'' and D (D $\epsilon C^{N_R\times N_T}$) act as a direct channel between the ''transmitter and receiver''. These corresponding channel matrices from Equations 2 to 4 as given in [24] are based on IRS-based MIMO models. In these equations, γ, $\bar{\gamma}$, and $\tilde{\gamma}$, denotes the normalization factors. β, $\bar{\beta}$, and $\tilde{\beta}$ denotes complex form of distributed Gaussian gain. L indicates attenuation in the propagated paths. G_e indicates IRS elemental gain. $a\left(\emptyset^i, \theta^i\right)$ represent the response vectors for azimuth angle $\emptyset^i$ and elevation angle θ^i where i is a corresponding path $i \in \{Tx, Rx, T-R, T-RIS, RIS-R\}$. H_{LOS}, G_{LOS}, D_{LOS} are the LOS components of sub channel.

Algorithm 1 Computation of IRS channel

Start

1. **Inputs** → $N_t, N_r IRS_{ele}$, H, G, D, β, θ
2. **Outputs** → $IRS_{channel}$
3. **Initialize parameters**
   a) N_t, N_r → number of Tx/ Rx antennas
   b) IRS_{ele} → number of IRS elements
4. **Generate channel matrix coefficients** → (H $\epsilon C^{N\times N_T}$), (G $\epsilon C^{N_R\times N}$), (D $\epsilon C^{N_R\times N_T}$)
5. **Generate diagonal matrix** → $\emptyset = diag\left(\beta e^{j\theta_1}, \ldots\ldots, \beta e^{j\theta_N}\right)$
6. **Calculate channel matrix** $\boldsymbol{IRS_{channel}}$ $IRS_{channel} = G\emptyset H + D$

End

Accordingly, end-to-end channel matrix (h_{IRS}) for an IRS-assisted MIMO system represented in Equation 5 [24].

$$h_{IRS} = G\emptyset H + D \tag{5}$$

When the signal gets transmitted through an IRS-based MIMO channel, it is influenced by the physical properties of the IRS and the surrounding environment. IRS enables the incoming signals in taking multiple paths to reach the receiver through scattering, diffraction, reflection and refraction. During the process, numerous copies of similar signals are received due to the multiple paths created. These components are partitioned into ''in-phase'' (i.e., real) or ''quadrature-phase'' (i.e., imaginary) components. This signal received near the destination will always be the sum of these components [25].

Depicting the received signal with channel coefficient h_{IRS}, transmitted signal x and additive noise n as given by Equation 6 [26].

$$y = h_{IRS}x + n \tag{6}$$

h is denoted as combination of h_r and h_i as real/ imaginary components as given in Equation 7 [27]

$$h_{IRS} = h_r + jh_i \tag{7}$$

Equations (6) and (7) are expressed in terms of MIMO systems, consisting N_t transmitter antennas, N_r receiver antennas having N_tN_r links between transmitter/receiver and channel with $N_r \times N_t$ dimensions. The received signal depicted for this case is given by Equation 8 [27], [28].

$$\begin{bmatrix} y_1 \\ y_2 \\ . \\ . \\ y_{N_r} \end{bmatrix} = \begin{bmatrix} h_{11} & h_{12} & \ldots & h_{1N_t} \\ h_{21} & h_{22} & \ldots & h_{2N_t} \\ : & : & \ldots & : \\ : & : & \ldots & : \\ h_{N_r1} & h_{N_r2} & \ldots & h_{N_rN_t} \end{bmatrix} \begin{bmatrix} x_1 \\ x_2 \\ : \\ : \\ x_{N_t} \end{bmatrix} + \begin{bmatrix} n_1 \\ n_2 \\ : \\ : \\ n_{N_r} \end{bmatrix} \tag{8}$$

y_i is the received signal and x_i be the transmitted signal at the i^{th} antenna. Complex channel coefficient h_{ij} acts as wireless link between transmitter/ receiver antennas. Furthermore, IRS-assisted MIMO channel is illustrated in Algorithm 1.

B. NONLINEAR MODEL

The purpose of considering nonlinear channels in any wireless environment is that, nonlinear channels results in varying levels of interference across different locations. As a result, it is essential to consider spatial correlation of the channel. Thus, wireless environment present unique behaviour when incorporates nonlinear distortion and considering IRS channel in such environments accurately represent the challenges faced in practical communication scenarios.

1) NONLINEAR DISTORTION

This article focuses on ''memoryless nonlinear models'' for estimating the distortion of the signal at the output, using a power-series technique from [12] expressed in Equation 9.

$$y(t) = \sum_{n=1}^{N} \alpha_n x^n(t) \tag{9}$$

Complex coefficients are denoted as α_n. $y(t)$ and $x(t)$ is a complex envelope of output and input signals. Moreover, from [12] nonlinear output $y_{dist}(t)$ is expressed as the sum of correlated $y_c(t)$ and uncorrelated $y_c(t)$ components which is depicted in Equations 10-12.

$$y_{dist}(t) = y_c(t) + y_d(t) \tag{10}$$

where,

$$y_c(t) = c_1 u_1(t) \tag{11}$$

$$y_d(t) = \sum_{n=2}^{N} c_n u_n(t) \tag{12}$$

''Nonlinear component'' is depicted as u_n, and c_n represents the envelope coefficients of the model. Input signal $u(t) = x(t)$, represents the nonlinear effects in terms of coefficient c_1 results in gain compression. Thus, system BER and SNR within signal bandwidth can be calculated as illustrated in algorithm 3.

$$R_{yy}(\tau) = R_{y_c y_c}(\tau) + R_{y_d y_d}(\tau) \tag{13}$$

Furthermore, PSD is utilized as a means of quantifying nonlinear distortion which employs FT of the ''autocorrelation function'' of output in the ''nonlinear model''. Utilizing Equation 10, the autocorrelation can be denoted as shown in Equation 13 [12] and PSD of the required nonlinear output is achieved when Equation 13 undergoes FT. This is indicated in Equation 14.

$$S_{yy}(f) = S_{y_c y_c}(f) + S_{y_d y_d}(f) \tag{14}$$

$S_{y_d y_d}(f)$ and $S_{y_c y_c}(f)$ are the PSD of useful/ undistorted components of the nonlinear output and further illustrated using algorithm 2.

Algorithm 2 Computation of PSD

Start

1. **Inputs** → $x, c_n, IRS_{ele}, N_t, N_r, mod_{ord}$, N, B, E_b/N_0
2. **Output** → $y_{dist}, S_{y_c y_c}, S_{y_d y_d}$
3. **Initialize parameters**
   a) N_t, N_r → Number of Tx/ Rx antennas
   b) IRS_{ele} → Number of IRS elements
   c) c_n → Envelope coefficients
   d) mod_{ord} → Modulation order
   e) N → Number of Simulations
   f) B → Bandwidth
   g) E_b/N_0 → SNR range
3. **Generate correlated/ uncorrelated components** → $y_c(t) = c_1 u_1(t)\,; y_d(t) = \sum_{n=2}^{N} c_n u_n(t)$
4. **Compute nonlinear output y_{dist}** → $y_{dist}(t) = y_c(t) + y_d(t)$
5. **Compute PSD of y_{dist}** → $R_{yy}(\tau) = R_{y_c y_c}(\tau) + R_{y_d y_d}(\tau)$
6. **Compute FT of → $R_{yy}(\tau)$** $S_{yy}(f) = S_{y_c y_c}(f) + S_{y_d y_d}(f)$
7. **Analyze the Output** → Power spectrum (dB/Hz) Vs Frequency

End

2) NON-IID GAUSSIAN

Non-IID channels encounters varying levels of interference across different locations. Especially, with the addition of nonlinear distortion, a non-Gaussian noise gets introduced to the system, analysing the channel's behaviour is crucial for alleviating co-channel interference. Initially, to model the noise with non-Gaussian nature, the ''ε-contaminated model'' as represented in Equation 15 [29] is employed.

$$p = (1-\varepsilon)\mathcal{N}(0, k_1) + \varepsilon\mathcal{N}(0, k_2) \tag{15}$$

p defines ''probability distribution of noise'' and $\varepsilon \in (0, 1)$ denotes the ''degree of contamination'', $\mathcal{N}(\mu, k)$ represents the Gaussian distribution with mean μ and covariance Σ. The presence of correlation at the transmitter is modelled as (R_{Tx}) and receive correlation as (R_{Rx}) matrices. Correlation between these channel components occur frequently in IRS-assisted MIMO communication systems as antenna spacing at the transmitter or receiver can result in spatially correlated channel characteristics between co-located antennas.

Expressing Correlation between signals from any antenna elements m, n within an array is denoted as $R_{(m,n)}$. The realization of channel correlated conditions is based on the ''Kronecker model'' [30] as indicated in Equation 16. Furthermore, the phase distribution component is highlighted by Equation 17 is obtained from [31], where $\Gamma(.)$ denotes the Gamma function and ϖ is a random variable.

$$H_C = R_{Rx}^{1/2} H R_{Tx}^{1/2} \tag{16}$$

$$p(\emptyset) = \frac{2m^m \varpi^{2m-1}}{\Gamma(m)} e^{(-m\varpi^2)} \tag{17}$$

Algorithm 3 Computing the performance of IRS-assisted channel in terms of BER vs SNR

Start

1. **Inputs** → $N_t, N_r IRS_{ele}$, H, G, D, mod_{ord}, N, X, E_b/N_0
2. **Output** → BER_{QPSK} / BER_{16-QAM}
3. **Initialize parameters**
   a) N_t, N_r → transmit/ receiver antennas
   b) X → Input Signal
   c) mod_{ord} → modulation order (QPSK, 16QAM)
   d) E_b/N_0 → SNR in dB
   e) N → number of simulations
4. **For mIndex** → 1 : length (M)
   Spatial multiplexing
   for snrIndex→ 1 : length (E_b/N_0)
   SNR ← E_b/N_0 (snrIndex);
   $error_{IID}$ ← 0; $error_{non-IID}$ ← 0
   for sim→ 1 : N
   n_{IID}; $n_{non-IID}$ % noise generation
   $H_C \leftarrow R_{Rx}^{1/2} H R_{Tx}^{1/2}$ % Kronecker model
   $p(\emptyset) \leftarrow \frac{2m^m \varpi^{2m-1}}{\Gamma(m)} e^{\left(-m\varpi^2\right)}$ % phase
   $y_{IID} \leftarrow channel_{IID} * X + n_{IID}$
   $y_{non-IID} \leftarrow$
   $channel_{non-IID} * X + n_{non-IID}$
   $y_{dist}(t) \leftarrow y_c(t) + y_d(t)$
   End
   End
   Symbol detection and BER calculations
   BER ← $error/(N * N_t)$
   End
5. **Analyze the performance**
   BER Vs SNR
   % BER_{QPSK}, BER_{16-QAM}
   → IID Gaussian/ non-IID Gaussian case
   → Nonlinear distortion case

End

Algorithm 4 Computing the performance of IRS-assisted MIMO in terms of Ergodic channel capacity vs SNR

Start

1. **Inputs** → $N_t, N_r IRS_{ele}$, H, G, D, N, X, E_b/N_0
2. **Output** → $Capacity_{IID}$, $Capacity_{non-IID}$, $Capacity_{dist}$
3. **Initialize parameters**
   a) N_t, N_r → transmit/ receiver antennas
   b) X → Input Signal
   c) E_b/N_0 → SNR in dB
   d) N → number of simulations
4. **For mIndex**→ 1 : length (M)
   Spatial multiplexing
   for snrIndex→ 1 : length (E_b/N_0)
   SNR ← E_b/N_0 (snrIndex);
   $error_{IID}$ ← 0; $error_{non-IID}$ ← 0
   for sim→ 1 : N
   n_{IID}; $n_{non-IID}$ % noise generation
   $H_C \leftarrow R_{Rx}^{1/2} H R_{Tx}^{1/2}$ % Kronecker model
   $p(\emptyset) \leftarrow \frac{2m^m \varpi^{2m-1}}{\Gamma(m)} e^{\left(-m\varpi^2\right)}$ % phase $y_{dist}(t)$
   ← $y_c(t) + y_d(t)$
   End
   End
   Channel capacity →
   C ← $\left\{\log_2 \left| \frac{\rho}{N_t} H H^H + I(N_r) \right| \right\}$
   End
5. **Analyze the performance** → channel capacity Vs SNR
   $Capacity_{IID}$, $Capacity_{non-IID}$, $Capacity_{dist}$

End

"Correlated channel matrix" is depicted by H_C and H is the channel matrix with dimensions of $N_r \times N_t$. Later, channel matrix H is replaced by the h_{IRS} that constitutes channel matrix coefficient G, H and D (as indicated in Equations 1-3) to analyse the behaviour of the channel in the presence of nonlinearity.

The introduction of nonlinearity in this work concentrates on analysing the behaviour of IRS assisted MIMO systems, as mentioned in Equations 9 to 11 which is shown to significantly alter the behaviour of the wireless channel. Furthermore, nonlinear distortions have more pronounced impact on IRS based MIMO systems as signal encoding near the transmitter results in higher interference in comparison to SISO systems.

The realistic observation of a nonlinear distorted IRS scheme gives intuition into the behavior over the correlated Rayleigh fading channel. This fading scenario offers larger SNR variations, creating negative impact on the channel performance and discourages the utilization of i.i.d. Rayleigh fading model [32].

Despite the challenges offered by nonlinear distortions, adopting suitable transmission technique becomes predominant. This study employs MIMO spatial multiplexing scheme due to its potential for capacity improvements compared to traditional single-antenna transmission schemes. Spatial multiplexing-based IRS system contributes an additional spatial dimension and yields a higher "degree-of-freedom" during communication. This increases diversity order, enhancing reliability in the fading scenarios, which is beneficial for achieving higher data rates and, consequently, greater capacity.

Since "ML detection" is the optimal decoding scheme [33] and the same is followed for detecting spatially multiplexed systems, yielding symbol vector $\hat{x}$ as indicated in Equation 18 where X is the set of symbol vector that are transmitted and y is the received symbol vector.

$$\hat{x} = \arg\max_{x \in X} \|y - HX\|^2 \tag{18}$$

Lastly, the performance is analysed in terms of two performance metrices mainly channel capacity and BER. The "channel capacity" (C) can be computed by utilizing

Equation 19 from [24] and [34].

$$C = \left\{ \log_2 \left| \frac{\rho}{N_t} HH^H + I\left(N_r\right) \right| \right\} \tag{19}$$

SNR is represented by ρ and H^H is a conjugate transpose of the vector H. Additionally, algorithm 4 illustrates the computation of ergodic channel capacity vs SNR.

III. SIMULATION RESULTS AND DISCUSSION

This article presents an insight by considering the nonlinear distorted and spatially correlated channel effects over an IRS-based SMX system. Understanding the implications of nonlinear effects in wireless environments is crucial due to variations of interference in distinct locations. It is imperative to consider the spatial correlation of the channel and assess the performance to analyze the influence of nonlinear distortions and system behavior over IID and non-IID Gaussian channel variations in indoor and outdoor scenarios. Despite these complexities associated with nonlinear distortions, the utilization of the MIMO SMX scheme is particularly significant due to its ability to provide an additional spatial diversity during transmission. This factor enhances reliability in correlated fading scenario, by enabling higher data rates and improved channel capacity.

This section is devoted to the description for analyzing the performance investigation of IRS based MIMO SMX scheme in realistic fading scenarios. ''Monte Carlo simulations'' have been carried out with a minimum of 10^6 channel realizations. The BER values are plotted against SNR to examine the behavior of the IRS-assisted MIMO channel using two modulation schemes: QPSK and 16 QAM. Two configurations of IRS elements, 4 and 16, are chosen for implementation in 4×4 MIMO systems. The bandwidth adheres to the 3GPP FR1 band standards, and the simulation encompasses both outdoor and indoor environments.

A. POWER SPECTRAL DENSITY

PSD vs. frequency plots provide significant insights into the signal characteristics, revealing the asymmetrical shapes or non-smoother behaviors which indicates distortions. By investigating the distribution of power across various frequencies, the presence of distortion can be identified, and also gain insights into their underlying issues. As a part of this article, PSD was computed utilizing the FT of the ''autocorrelation function'' of the output, as depicted in Equation 13.

From Figure 2, it is observed that, PSD vs Frequency, for uncorrelated channel realizations, spectrum resembles the Gaussian distribution which remain flat across the signal bandwidth. The resemblance arises from CLT, indicating no discernible patters across different frequency components. This is due to dependencies between signals at different frequencies. However, in correlated spectrum with IRS are likely to introduce distortion than uncorrelated channels due to larger variations in the power across different frequencies. Additionally, the spatial correlation of reflective elements is

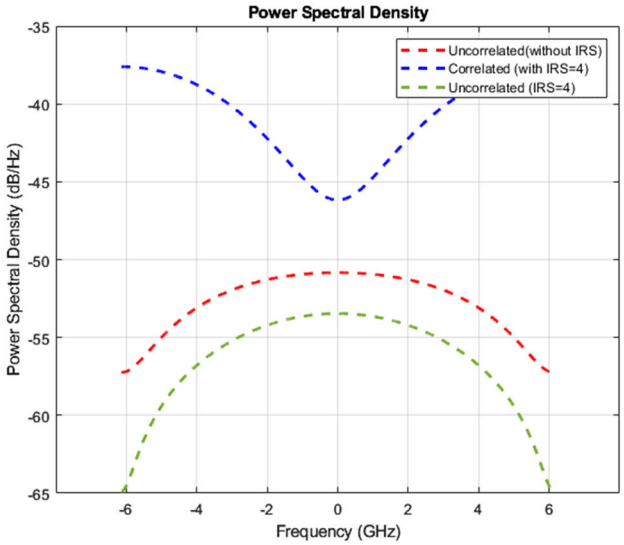

FIGURE 2. PSD of nonlinear output partitioned as correlated and uncorrelated with IRS.

significant, as IRS can selectively enhance specific frequency components based on the phase shifts induced by elements.

B. BER VERSUS SNR

Furthermore, to achieve a BER of 10^{-5} over a non-IID Gaussian channel, an SNR of 5 dB is required for a system which employs 16 elements of IRS. Same pattern is observed for the system which constitutes 4 elemental IRS which produces the prescribed BER of 10^{-5} for an SNR of 15dB. Figure 3, also demonstrates the effect of nonlinear distorted IRS scheme (N = 16) for the above BER at an SNR of −6dB. The realistic observation on nonlinear distorted IRS scheme gives intuition into the behavior over Rayleigh outdoor channel. This uniqueness lies in understanding that, even though the channel is distorted nonlinearly, the BER performance is very much closer to IID Gaussian case. Performance deterioration is generally observed in Non-IID Gaussian channels which has non-uniform phase [31] parameters.

From Figure 4, for a 4× 4 MIMO SMX set up utilizing QPSK modulation, achieving a BER of 10^{-5} requires an SNR of −15dB with IID-Gaussian realizations (IRS = 16). In order to achieve the same BER, IID-Gaussian channel operating with IRS = 4 elements, require around −5 dB SNR. This observation underlines the efficacy of incorporating higher reflecting elements, precisely steering the energy of the signals and thus reducing SNR requirements. Moreover, to attain BER of 10^{-5} over a non-IID Gaussian channel, an SNR of 0 dB is needed for a system employing 16 IRS elements. Similarly, with 4 elemental setups, attain the same BER at an SNR of 10dB.

Figure 4, illustrates the impact of nonlinear distorted IRS scheme (N = 16) on the aforementioned BER at an SNR of −10dB. The empirical insight into nonlinear distorted channel sheds light on its behavior over Rician dominant

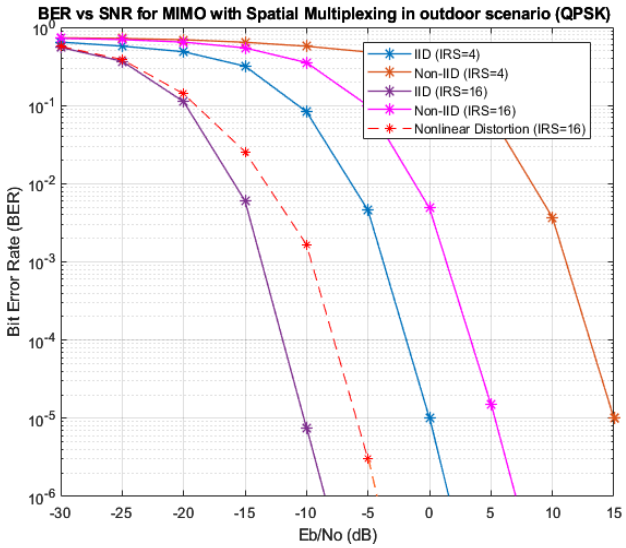

FIGURE 3. Plot of BER Vs SNR with SMX in IID-Gaussian/ Non-IID Gaussian channel and nonlinear distortion for QPSK modulation scheme in outdoor scenario.

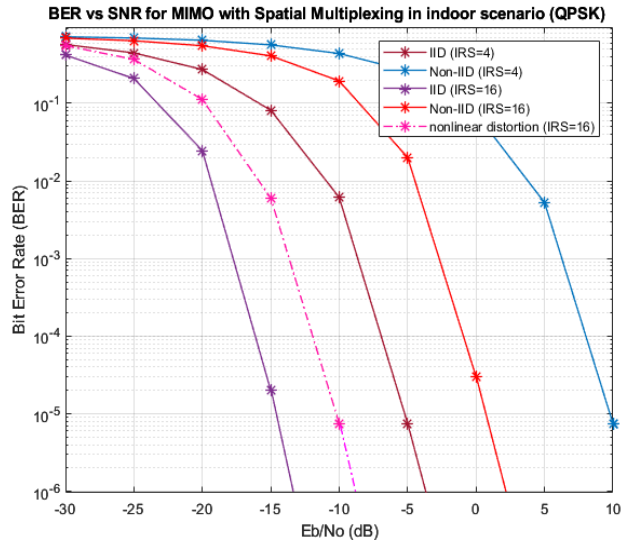

FIGURE 4. Plot of BER Vs SNR with SMX in IID-Gaussian/ Non-IID Gaussian channel and nonlinear distortion for QPSK modulation scheme in indoor scenario.

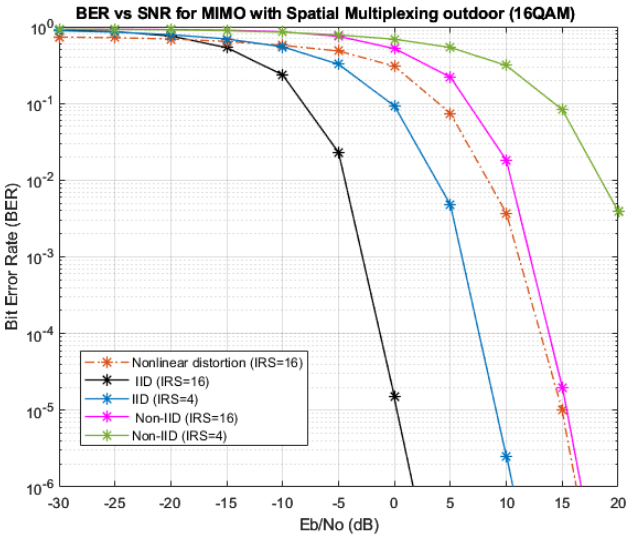

FIGURE 5. Plot of BER Vs SNR with SMX in IID-Gaussian/ Non-IID Gaussian channel and nonlinear distortion for 16QAM modulation scheme in outdoor scenario.

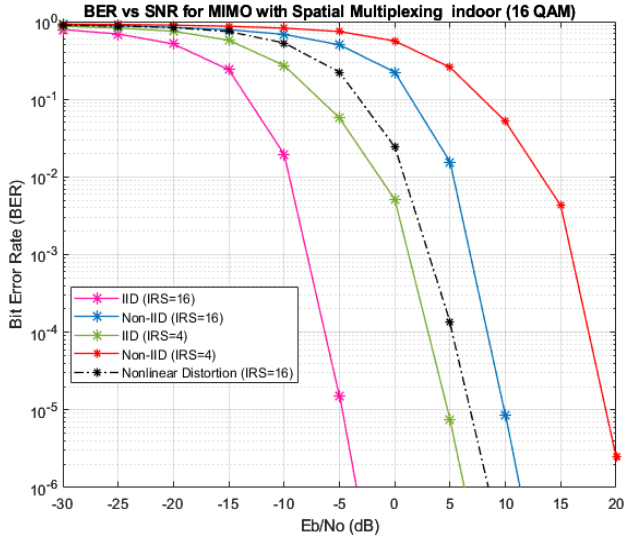

FIGURE 6. Plot of BER Vs SNR with SMX in IID-Gaussian/ Non-IID Gaussian channel and nonlinear distortion for 16QAM modulation scheme in indoor scenario.

channels, particularly in indoor settings. It is noteworthy that despite the nonlinear distorted IRS scheme, The BER performance closely aligns with IID Gaussian case. Furthermore, to attain the BER of 10^{-5} in nonlinear distorted channels (N = 16) of Rayleigh outdoor scheme (as shown in Figure 3), an SNR of −6dB is required. To achieve a similar BER by the Rician dominant indoor setup (as shown in Figure 4), an SNR of approximately −10dB is required implying that Rayleigh dominant channels demands higher SNR and introduces more significant challenges to the channel comparatively.

For a 4× 4 MIMO SMX systems employing 16 QAM modulation in outdoor scenario (as shown in Figure 5), attaining the BER of 10^{-5} demands an SNR of 0 dB for an IID-Gaussian channel with 16 IRS elements. However, to achieve aforementioned BER for an IID-Gaussian with 4 IRS elements, a higher SNR of approximately 7 dB higher SNR is needed. This observation suggests that increasing the number of reflecting elements indeed contributes to enhanced signal directionality and consequently reduces SNR. Furthermore, to attain a BER of 10^{-5} over a non-IID Gaussian channel, an SNR of 15 dB is necessary for a system employing 16 IRS elements. A similar pattern is followed that constitutes 4 IRS elements which achieves the BER of 10^{-5} at an SNR of 25 dB. Additionally, Figure 5 illustrates the effect of nonlinear distorted IRS scheme (N = 16) on the aforementioned BER at an SNR of 14dB.

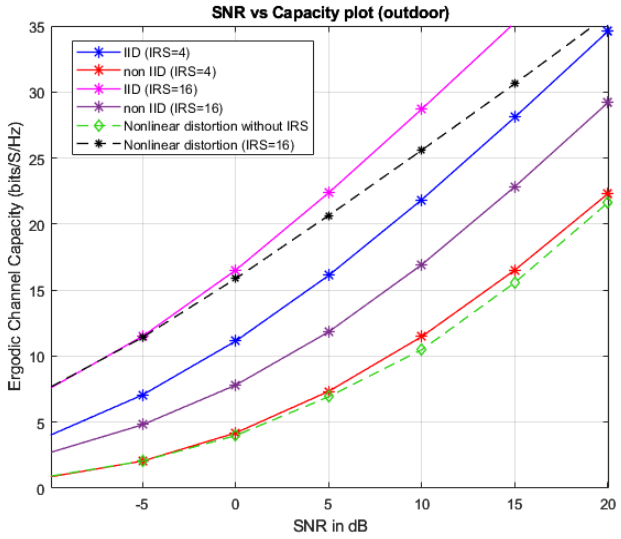

FIGURE 7. Plot of Ergodic channel capacity Vs SNR.

For an indoor scenario of 4×4 MIMO SMX systems employing 16 QAM modulation (as shown in Figure 6), achieving a BER of approximately 10^{-5} requires an SNR of -5 dB for the IID-Gaussian (IRS = 16) setup. For an IID-Gaussian (IRS = 4) configuration to match this BER, an SNR of approximately 10 dB higher, which is observed at 5dB. Furthermore, to attain a BER of 10^{-5} over a non-IID Gaussian channel, a system employing 16 elemental IRS demands an SNR of 10dB. Similarly, a system with 4 IRS elements achieves the same BER at an SNR of 18dB. Additionally, Figure 6 illustrates the influence of nonlinear distorted IRS scheme with 16 IRS elements on the aforementioned BER at an SNR of 7dB.

C. ERGODIC CHANNEL CAPACITY VERSUS SNR

This section elucidates the influence of IRS in analysing the ergodic channel capacity under the conditions encompassing IID-Gaussian/ non-IID Gaussian and in-band nonlinear distortions.

In Figure 7, it is apparent that in a 4× 4 MIMO SMX configuration, IID-Gaussian channels with 16 elemental IRS exhibits channel capacity of up to 35 bits/s/Hz at a highest SNR of 15dB. Achieving a comparable performance with 4 elemental IRS demands additional 5 dB i.e., up to 20 dB of SNR. This emphasizes the importance of having higher number of IRS elements, enabling finer control over signal reflection properties, thereby improving the achievable capacity even at lower SNRs. Accordingly, non-IID Gaussian channels with 16 elemental IRS demonstrate channel capacity of up to 23bits/s/Hz at a 15 dB SNR. To attain a similar performance in 4 elemental IRS, an SNR of 20dB is required. Additionally, Figure 7 depicts the impact of nonlinear distorted channels with 16 IRS elements, yielding 20bits/s/Hz at 5 dB SNR, which aligns with the performance of IID-Gaussian case. Achieving a similar capacity without the use of IRS requires additional SNR of ∼20 dB, which indicates the importance of IRS in mitigating the effects of nonlinear distortion effects by improving the achievable capacity at lower SNR.

IV. CONCLUSION

This paper investigates the performance of IRS-assisted MIMO-SMX systems, focusing on the impact of nonlinear distortions and system behaviour across IID and non-IID Gaussian channel scenarios. The Monte Carlo simulations are employed to assess the BER performance and to characterize correlated/uncorrelated channel conditions. These simulations aim to provide quantitative insights into wireless system behaviour, analysing Ergodic Channel capacity vs SNR in the presence of IID-Gaussian/ non-IID Gaussian and in-band nonlinear distortions. Moreover, in densely correlated and practical channel conditions, it is observed that increasing the number of IRS elements enhances the BER performance by 8dB in both IID and non-IID Gaussian scenarios. Additionally, a noteworthy improvement of 5bps/Hz in ergodic channel capacity is observed at a fixed SNR of 5dB. Consequently, the simulation results emphasize the importance of exploring the limits of nonlinearity to develop precise realistic channel scenario that accurately capture frequency-selective fading, noise characterization, and other key properties for IRS-assisted MIMO systems.

REFERENCES

[1] C. Pan, H. Ren, K. Wang, J. F. Kolb, M. Elkashlan, M. Chen, M. Di Renzo, Y. Hao, J. Wang, A. L. Swindlehurst, X. You, and L. Hanzo, "Reconfigurable intelligent surfaces for 6G systems: Principles, applications, and research directions," *IEEE Commun. Mag.*, vol. 59, no. 6, pp. 14–20, Jun. 2021, doi: 10.1109/MCOM.001.2001076.

[2] M. Di Renzo, K. Ntontin, J. Song, F. H. Danufane, X. Qian, F. Lazarakis, J. De Rosny, D.-T. Phan-Huy, O. Simeone, R. Zhang, M. Debbah, G. Lerosey, M. Fink, S. Tretyakov, and S. Shamai (Shitz), "Reconfigurable intelligent surfaces vs. relaying: Differences, similarities, and performance comparison," *IEEE Open J. Commun. Soc.*, vol. 1, pp. 798–807, 2020, doi: 10.1109/OJCOMS.2020.3002955.

[3] Z. Chen, X. Ma, C. Han, and Q. Wen, "Towards intelligent reflecting surface empowered 6G terahertz communications: A survey," *China Commun.*, vol. 18, no. 5, pp. 93–119, May 2021, doi: 10.23919/JCC.2021.05.007.

[4] T. Araújo and R. Dinis, *Analytical Evaluation of Nonlinear Distortion Effects on Multicarrier Signals*. Boca Raton, FL, USA: CRC Press, 2015.

[5] K. M. Gharaibeh, K. Gard, and M. B. Steer, "The impact of nonlinear amplification on the performance of CDMA systems," in *Proc. IEEE Radio Wireless Conf.*, Feb. 2005, pp. 83–86, doi: 10.1109/rawcon.2004.1389077.

[6] B. Sklar, "Rayleigh fading channels in mobile digital communication systems. I. Characterization," *IEEE Commun. Mag.*, vol. 35, no. 7, pp. 90–100, Jul. 1997, doi: 10.1109/35.601747.

[7] V. Abramova, V. Lukin, S. Abramov, K. Abramov, and E. Bataeva, "Analysis of statistical and spatial spectral characteristics of distortions in lossy image compression," in *Proc. IEEE 2nd Ukrainian Microw. Week (UkrMW)*, Nov. 2022, pp. 644–649, doi: 10.1109/UkrMW58013.2022.10036949.

[8] M. Shehata, K. Wang, J. Webber, M. Fujita, T. Nagatsuma, and W. Withayachumnankul, "Timing-jitter tolerant Nyquist pulse for terahertz communications," *J. Lightw. Technol.*, vol. 40, no. 2, pp. 557–564, Jan. 15, 2022, doi: 10.1109/JLT.2021.3121814.

[9] B. He and F. Wang, "Cooperative specific emitter identification via multiple distorted receivers," *IEEE Trans. Inf. Forensics Security*, vol. 15, pp. 3791–3806, Jan. 2020, doi: 10.1109/TIFS.2020.3001721.

[10] K. M. Gharaibeh, K. G. Gard, and M. B. Steer, "Estimation of co-channel nonlinear distortion and SNDR in wireless systems," *IET Microw., Antennas Propag.*, vol. 1, no. 5, p. 1078, Jan. 2007, doi: 10.1049/iet-map:20070034.
[11] K. M. Gharaibeh, K. G. Gard, and M. B. Steer, "In-band distortion of multisines," *IEEE Trans. Microw. Theory Techn.*, vol. 54, no. 8, pp. 3227–3236, Aug. 2006, doi: 10.1109/TMTT.2006.879170.
[12] K. M. Gharaibeh, "The effect of nonlinear distortion on the performance of MIMO systems," *AEU Int. J. Electron. Commun.*, vol. 69, no. 2, pp. 555–561, Feb. 2015, doi: 10.1016/j.aeue.2014.11.006.
[13] K. M. Gharaibeh, *Nonlinear Distortion in Wireless Systems: Modeling and Simulation With MATLAB*. Chichester, U.K.: Wiley, 2011.
[14] R. Ma, J. Tang, X. Y. Zhang, K.-K. Wong, and J. A. Chambers, "RIS-assisted SWIPT network for Internet of everything under the electromagnetics-based communication model," *IEEE Internet Things J.*, vol. 11, no. 9, pp. 15402–15415, May 2024, doi: 10.1109/JIOT.2023.3347623.
[15] J. Lee and K. Yang, "RF power analysis on 5.8 GHz low-power amplifier using resonant tunneling diodes," *IEEE Microw. Wireless Compon. Lett.*, vol. 27, no. 1, pp. 61–63, Jan. 2017, doi: 10.1109/LMWC.2016.2629984.
[16] P. Banelli and S. Cacopardi, "Theoretical analysis and performance of OFDM signals in nonlinear AWGN channels," *IEEE Trans. Commun.*, vol. 48, no. 3, pp. 430–441, Mar. 2000, doi: 10.1109/26.837046.
[17] Z. Zhu, N. Wang, W. Hao, Z. Wang, and I. Lee, "Robust beamforming designs in secure MIMO SWIPT IoT networks with a nonlinear channel model," *IEEE Internet Things J.*, vol. 8, no. 3, pp. 1702–1715, Feb. 2021, doi: 10.1109/JIOT.2020.3014933.
[18] X. Pan, X. Wang, B. Tian, C. Wang, H. Zhang, and M. Guizani, "Machine-learning-aided optical fiber communication system," *IEEE Netw.*, vol. 35, no. 4, pp. 136–142, Jul. 2021, doi: 10.1109/MNET.011.2000676.
[19] D. Kakati and S. C. Arya, "A 640-Gbps, 15.2344-b/s/Hz full-duplex optical fiber/wireless single-channel coherent communication system using IQM-based DP-256-QAM and DSP techniques," *Photonic Netw. Commun.*, vol. 39, no. 1, pp. 26–38, Dec. 2019, doi: 10.1007/s11107-019-00875-7.
[20] S. Shimizu, T. Kazama, T. Kobayashi, T. Umeki, K. Enbutsu, R. Kasahara, and Y. Miyamoto, "Accurate estimation of chromatic dispersion for non-degenerate phase-sensitive amplification," *J. Lightw. Technol.*, vol. 39, no. 1, pp. 24–32, Jan. 1, 2021, doi: 10.1109/JLT.2020.3022871.
[21] D. Wang, Y. Song, J. Li, J. Qin, T. Yang, M. Zhang, X. Chen, and A. C. Boucouvalas, "Data-driven optical fiber channel modeling: A deep learning approach," *J. Lightw. Technol.*, vol. 38, no. 17, pp. 4730–4743, Sep. 15, 2020, doi: 10.1109/JLT.2020.2993271.
[22] M. Wennström, "On MIMO systems and adaptive arrays for wireless communications: Analysis and practical aspects," M.S. thesis, Dept. Mater. Sci., Distrib. Signals Syst., Uppsala Univ., Uppsala, Sweden, Elanders Gotab AB, Stockholm, Sweden, Sep. 2002, p. 291.
[23] M. Torbatian, D. Lavery, M. Osman, D. Yao, D. S. Millar, Y. Gao, A. Kakkar, Z. A. El-Sahn, C. Doggart, A. E. Morra, N. Abughalieh, S. Yang, X. Chen, R. Maher, H. Sun, K.-T. Wu, and P. Kandappan, "Performance oriented DSP for flexible long haul coherent transmission," *J. Lightw. Technol.*, vol. 40, no. 5, pp. 1256–1272, Mar. 1, 2022, doi: 10.1109/JLT.2021.3134155.
[24] E. Basar and I. Yildirim, "Reconfigurable intelligent surfaces for future wireless networks: A channel modeling perspective," *IEEE Wireless Commun.*, vol. 28, no. 3, pp. 108–114, Jun. 2021, doi: 10.1109/MWC.001.2000338.
[25] T. S. Rappaport, *Wireless Communications: Principles and Practice*, vol. 2. Upper Saddle River, NJ, USA: Prentice-Hall, 1996.
[26] A. Papoulis and S. U. Pillai, *Probability, Random Variables, and Stochastic Processes*. New York, NY, USA: Tata McGraw-Hill Education, 2002.
[27] A. L. Imoize, A. E. Ibhaze, A. A. Atayero, and K. V. N. Kavitha, "Standard propagation channel models for MIMO communication systems," *Wireless Commun. Mobile Comput.*, vol. 2021, pp. 1–36, Feb. 2021, doi: 10.1155/2021/8838792.
[28] J. Choi, D. J. Love, and P. Bidigare, "Downlink training techniques for FDD massive MIMO systems: Open-loop and closed-loop training with memory," *IEEE J. Sel. Topics Signal Process.*, vol. 8, no. 5, pp. 802–814, Oct. 2014, doi: 10.1109/JSTSP.2014.2313020.
[29] Z. Li, S. Li, B. Liu, S. S. Yu, and P. Shi, "A stochastic event-triggered robust cubature Kalman filtering approach to power system dynamic state estimation with non-Gaussian measurement noises," *IEEE Trans. Control Syst. Technol.*, vol. 31, no. 2, pp. 889–896, Mar. 2023, doi: 10.1109/TCST.2022.3184467.
[30] G. D. G. Simha, S. Koila, N. Neha, M. A. N. S. Raghavendra, and U. Sripati, "Redesigned spatial modulation for spatially correlated fading channels," *Wireless Pers. Commun.*, vol. 97, no. 4, pp. 5003–5030, Aug. 2017, doi: 10.1007/s11277-017-4762-6.
[31] M. D. Yacoub, "Nakagami-*m* phase–envelope joint distribution: A new model," *IEEE Trans. Veh. Technol.*, vol. 59, no. 3, pp. 1552–1557, Mar. 2010, doi: 10.1109/TVT.2010.2040641.
[32] E. Björnson and L. Sanguinetti, "Rayleigh fading modeling and channel hardening for reconfigurable intelligent surfaces," *IEEE Wireless Commun. Lett.*, vol. 10, no. 4, pp. 830–834, Apr. 2021, doi: 10.1109/LWC.2020.3046107.
[33] G. D. G. Simha, S. Koila, R. Mans, and U. Sripati, "Modified signal design for multistream spatial modulation over spatially correlated channels," in *Proc. Int. Conf. Adv. Comput., Commun. Inform. (ICACCI)*, Sep. 2017, pp. 612–617, doi: 10.1109/ICACCI.2017.8125908.
[34] T. Van Chien, L. T. Tu, S. Chatzinotas, and B. Ottersten, "Coverage probability and ergodic capacity of intelligent reflecting surface-enhanced communication systems," *IEEE Commun. Lett.*, vol. 25, no. 1, pp. 69–73, Jan. 2021, doi: 10.1109/LCOMM.2020.3023759.

D. L. SHARINI received the Bachelor of Engineering degree in electronics and communication engineering from Visvesvaraya Technological University, Belgaum, Karnataka, India, in 2019, and the Master of Technology degree in control systems engineering from Manipal Institute of Technology (MIT), Manipal, Karnataka, India, in 2021, where she is currently pursuing the Ph.D. degree in electronics and communication engineering. Her specializations include wireless communications, intelligent reflecting surface (IRS), massive MIMO technologies, millimeter-wave communications, and machine learning.

RAVILLA DILLI (Member, IEEE) received the Bachelor of Technology degree from Jawaharlal Nehru Technological University, Hyderabad, India, the Master of Engineering degree in applied electronics from Sathyabama University, and the Ph.D. degree from JNTUH, in 2018. He is currently an Associate Professor with the Department of Electronics and Communication Engineering, Manipal Institute of Technology, Manipal Academy of Higher Education, Manipal, Karnataka, India. He holds four best research paper awards to his credit and received an excellence award for internship as part of Samsung Prism. He has published 36 research papers in national and international journals and conference proceedings. He has 20 years of teaching and research experience in the fields of communication networks, network security, mobile communication systems, routing protocols and algorithms in mobile ad hoc networks (MANETs) and wireless sensor networks, vehicular ad hoc networks (VANETs), 5G and 6G wireless technologies, and the Internet of Things. As a Technical Program Committee Member, he has reviewed more than 160 research articles for Scopus/Web of Science journals, including *Wireless Networks*, IEEE Access, IEEE Transactions on Communications, IEEE Internet of Things Journal, *Wireless Personal Communications*, *International Journal of Electronics*, *Journal of Experimental and Theoretical Artificial Intelligence*, *International Journal of Wireless Information Networks*, *Indonesian Journal of Electrical Engineering and Computer Science*, *International Journal of Informatics and Communication Technology* (IJ-ICT), *International Journal of Electrical and Computer Engineering*, *International Journal of Computer Engineering Research*, *Sensors*, *Applied Sciences*, *Energies*, *Remote Sensing*, *Mathematics*, *Telecom*, *Electronics*, *Journal of Sensor and Actuator Networks*, *Entropy*, and international conferences sponsored by IEEE and Springer.

M. KANTHI (Member, IEEE) received the Bachelor of Technology degree from the Malnad College of Engineering, Hassan, the Master of Technology degree in digital electronics and communication engineering from NITK, Surathkal, Karnataka, and the Ph.D. degree from MAHE, Manipal, Karnataka, India, in 2014. She is currently a Professor with the Department of Electronics and Communication Engineering, Manipal Institute of Technology, Manipal Academy of Higher Education. She has published 15 research papers in national and international journals and conference proceedings. She has 25 years of teaching and research experience in the fields of microcontrollers and embedded systems, communication networks, system-on-chip design, embedded system design, ARM processor architecture, and embedded control systems. Her areas of research interests include real-time systems, artificial intelligence, embedded control systems, and wireless sensor networks for biomedical applications. As a technical program committee member, she has reviewed more than 20 research papers for Scopus/Web of Science journals and conferences.

G. D. GOUTHAM SIMHA (Member, IEEE) received the Ph.D. degree from the National Institute of Technology Karnataka, Surathkal, India, in 2018. He was an Intern with LEOS ISRO, Bangalore, for the project entitled "Design and Implementation of ATP Sensor for Optical Inter-Satellite Links," in 2008. He was a part of the "Uncoordinated Secure and Energy Aware Access in Distributed Wireless Networks" project, which was sponsored by the Information Technology Research Academy (ITRA) Media Lab Asia, in 2015. He was a Faculty Member with the Department of Electronics and Communication Engineering, NITK, from January 2018 to June 2019. Currently, he is an Associate Professor with the Department of Electronics and Communication Engineering, Manipal Institute of Technology, Manipal, Karnataka, India. His areas of research interests include spatial modulation, RIS communications, massive MIMO, optical wireless communications, and error control coding.